


Suppression of polaron self-localization by correlations

Lilith Zschetzsche and Robert E. Zillich *Institute for Theoretical Physics, Johannes Kepler University Linz, Altenberger Straße 69, 4040 Linz, Austria*

(Received 21 December 2023; accepted 4 April 2024; published 7 May 2024)

We investigate self-localization of a polaron in a homogeneous Bose-Einstein condensate in one dimension. This effect, where an impurity is trapped by the deformation that it causes in the surrounding Bose gas, has been first predicted by mean-field calculations, but has not been seen in experiments. We study the system in one dimension, where, according to the mean-field approximation, the self-localization effect is particularly robust and present for arbitrarily weak impurity-boson interactions. We address the question whether self-localization is a real effect by developing a variational method which incorporates impurity-boson correlations nonperturbatively and solving the resulting inhomogeneous correlated polaron equations. We find that correlations inhibit self-localization except for very strongly repulsive or attractive impurity-boson interactions. Our prediction for the critical interaction strength for self-localization agrees with a sharp drop of the inverse effective mass found in quantum Monte Carlo simulations of polarons in one dimension.

DOI: [10.1103/PhysRevResearch.6.023137](https://doi.org/10.1103/PhysRevResearch.6.023137)

I. INTRODUCTION

The original Bose polaron problem concerns an electron in a solid which is dressed by small distortions of the crystal lattice and was modelled by Fröhlich [1]. Another type of polaron is formed by an electron or impurity atom in superfluid ^4He . This problem has long been studied [2] and later extended to molecular impurities and impurity aggregates in ^4He , which lead to a new type of low-temperature spectroscopy of molecules [3,4]. More recently, polarons of mobile impurities have been experimentally realized in ultracold Bose gases [5–7].

For electrons in ionic solids [8] and in superfluid ^4He [9] a mechanism for self-localization, or self-trapping, was proposed [10]. Self-localization implies that, even in the absence of an external trap potential, the impurity probability density $\rho(\mathbf{r}_0)$ is not uniform but trapped by the distortion of the density of phonons or He atoms created by the impurity itself. In Refs. [11,12] based on the mean-field (MF) approach self-localization has also been predicted for polarons in a Bose-Einstein condensate. According to Cuccietti *et al.* [11] a polaron in a three-dimensional homogeneous Bose gas self-localizes above a critical impurity-boson interaction strength, while below it the polaron ground state is homogeneous. This would imply a phase transition to a translation symmetry-breaking ground state. Subsequently, other works have also predicted this effect, e.g., for neutral polarons, again using the MF approximation [13–17], including finite temperature calculations (using time-dependent Hartree-Fock-Bogoliubov [18] and Balian-Vénéroni variational principle [19]), and also

with other methods such as path integrals [20,21]. Also ionic polarons [22] and angular polarons [23] have been predicted to self-localize. However, other works have not seen evidence of self-localization in three dimensions [24–26], nor has it been observed experimentally. This raises the question whether self-localization is a methodological artifact or a real effect.

In one dimension the MF approximation predicts a self-trapped polaron regardless of the strength of the impurity-boson interaction [14]. Exact quantum Monte Carlo simulations [27] indeed predict an essentially divergent polaron effective mass above a certain impurity-boson interaction strength, i.e., the polaron becomes immobile, which would be consistent with self-localization for strong interactions. Conversely, Ref. [28] found a finite effective mass for attractive impurity-boson interaction, using the same Monte Carlo method for similar boson-boson interaction strengths but smaller mass ratio. Indirect measurements of Bose polarons in one dimension gave an even lower effective mass [5].

The goal of this work is to check if the self-localized ground state predicted by the MF approximation is a real effect or an artifact of the uncorrelated Hartree ansatz of MF. To check this, we take a crucial step beyond the Hartree ansatz by incorporating impurity-boson correlations in a non-perturbative way, while treating the weakly interacting Bose background still in the MF approximation, thus omitting boson-boson correlations. We note that the perturbative treatment of correlations (then usually referred to as quantum fluctuations) has been shown to lead to corrections to the density $\rho(x_0)$ of a self-localized impurity in one dimension [13] but still preserves self-localization. In this work we show that with a nonperturbative treatment of impurity-boson correlations impurity self-localization happens only for very strongly attractive or repulsive impurity-boson interactions.

Published by the American Physical Society under the terms of the [Creative Commons Attribution 4.0 International](https://creativecommons.org/licenses/by/4.0/) license. Further distribution of this work must maintain attribution to the author(s) and the published article's title, journal citation, and DOI.

II. THEORY AND METHOD

The Hamiltonian of one impurity and N bosons in one dimension is given by

$$H = -\frac{\hbar^2}{2M} \frac{\partial^2}{\partial x_0^2} - \frac{\hbar^2}{2m} \sum_{i=1}^N \frac{\partial^2}{\partial x_i^2} + \sum_{i=1}^N U(x_0 - x_i) + \lambda_{\text{BB}} \sum_{i<j} \delta(x_i - x_j) \quad (1)$$

consisting of the kinetic energy of the impurity, the kinetic energy of the bosons, the impurity-boson interaction, and the boson-boson interaction. The boson-boson interaction is modeled by a contact potential with strength λ_{BB} , which is related to the scattering length a_{BB} by $\lambda_{\text{BB}} = \frac{-2\hbar^2}{a_{\text{BB}}m}$ [29,30]. The impurity-boson interaction is modeled by a finite range potential, for which we choose a Gaussian, $U(x) = \frac{U_0}{2\sigma_U^2} \exp[-\frac{x^2}{\sigma_U^2}]$, characterized by the strength and width parameters U_0 and σ_U .

The MF approach is usually derived in a variational formulation, with the Hartree ansatz wave function for one impurity in a bath of N bosons:

$$\Psi_{\text{MF}} = \eta(x_0) \prod_{i=1}^N \psi(x_i). \quad (2)$$

This wave function does not account for the correlations caused by the interactions, e.g., the decrease of the probability $|\Psi(x_0, \dots, x_i, \dots)|^2$ if a boson at x_i is close to a repulsive impurity at x_0 . The optimization of Ψ_{MF} leads to one-body equations with effective potentials, the ‘‘mean fields.’’ The uncorrelated MF ansatz (2) can be expected to be a poor approximation of the true many-body wave function if impurity-boson interactions are strong (but our results show it is a poor approximation for weak interaction as well). Therefore, we generalize the ansatz by replacing the boson one-body functions $\psi(x_i)$ with impurity-boson *pair correlation* functions $f(x_0, x_i)$:

$$\Psi = \frac{1}{\Omega^{N/2}} \eta(x_0) \prod_{i=1}^N f(x_0, x_i), \quad (3)$$

where it turns out to be convenient to introduce a prefactor including the normalization volume Ω . This is a Jastrow-Feenberg ansatz wave function [31] but limited to impurity-boson correlations. We refer to it as the inhomogeneous correlated polaron (inh-CP) ansatz.

If the ground state is assumed homogeneous, i.e., translationally invariant like the Hamiltonian, the ansatz (3)

simplifies to

$$\Psi_{\text{hom}} = \frac{1}{\Omega^{(N+1)/2}} \prod_{i=1}^N f_{\text{hom}}(x_0 - x_i), \quad (4)$$

which was studied by Gross [32]. Of course, we cannot make this assumption of translational invariance if we want to study the possible symmetry breaking by self-localization of the impurity. But the homogeneous correlated polaron (hom-CP) ansatz (4) will still be useful: if self-localization is indeed energetically favorable, the energy difference between the inh-CP and the hom-CP result is the energy gained by forming a self-localized ground state.

Our ansatz (3) includes impurity-boson correlations but still treats the (weakly interacting) Bose background in the MF approximation, as it does not include boson-boson correlations. Since we take only one step beyond the MF approach, this allows for a comprehensible comparison between our method and the MF approach. Impurities immersed in a strongly interacting Bose liquid like ^4He , however, require the inclusion of boson-boson correlations. Optimizing such a full Jastrow-Feenberg ansatz leads to the hypernetted-chain Euler-Lagrange method [33,34]. The method and its time-dependent generalization have been used extensively to study impurities in ^4He [35–38].

Before deriving equations for $\eta(x_0)$ and $f(x_0, x_i)$ from the Ritz variational principle, we need an expression for the energy functional $E = \langle \Psi | H | \Psi \rangle$, where we assume normalization of the wave function, $\langle \Psi | \Psi \rangle = 1$. The four terms in the Hamiltonian (1) lead to the following four terms in E :

$$E = \frac{\hbar^2}{2M} \int d\mathbf{x} \left(\frac{\partial \Psi}{\partial x_0} \right)^2 + N \frac{\hbar^2}{2m} \int d\mathbf{x} \left(\frac{\partial \Psi}{\partial x_1} \right)^2 + N \int d\mathbf{x} \Psi^2 U(x_0 - x_1) + \frac{N(N-1)}{2} \int d\mathbf{x} \Psi^2 \lambda_{\text{BB}} \delta(x_1 - x_2), \quad (5)$$

where $d\mathbf{x} = dx_0 dx_1 \dots dx_N$, and Ψ is the correlated polaron ansatz (3). Owing to the star-shaped correlation structure, where the impurity is correlated with all bosons but the bosons are not correlated between themselves, most of the $N+1$ integrals in E factorize and yield $\int dx'_1 f(x_0, x'_1)^2$. We abbreviate this partially integrated correlation function

$$\bar{f}(x_0) \equiv \Omega^{-1} \int dx'_1 f(x_0, x'_1)^2. \quad (6)$$

We obtain the energy functional

$$E = \frac{\hbar^2}{2M} \left\{ \int dx_0 \left(\frac{\partial \eta(x_0)}{\partial x_0} \right)^2 \bar{f}(x_0)^N - \frac{N}{\Omega} \int dx_0 dx_1 \eta(x_0)^2 \bar{f}(x_0)^{N-1} f(x_0, x_1) \frac{\partial^2 f(x_0, x_1)}{\partial x_0^2} - \frac{N(N-1)}{\Omega^2} \int dx_0 \eta(x_0)^2 \bar{f}(x_0)^{N-2} \left[\int dx_1 f(x_0, x_1) \frac{\partial f(x_0, x_1)}{\partial x_0} \right]^2 \right\} + \frac{\hbar^2 N}{2m \Omega} \int dx_0 dx_1 \eta(x_0)^2 \bar{f}(x_0)^{N-1} \left(\frac{\partial f(x_0, x_1)}{\partial x_1} \right)^2 + \frac{N}{\Omega} \int dx_0 dx_1 \eta(x_0)^2 \bar{f}(x_0)^{N-1} f(x_0, x_1)^2 U(x_0, x_1) + \frac{\lambda_{\text{BB}} N(N-1)}{2 \Omega^2} \int dx_0 dx_1 \eta(x_0)^2 \bar{f}(x_0)^{N-2} f(x_0, x_1)^4. \quad (7)$$

In a study of self-localization, we are primarily interested in the impurity density $\rho_I(x_0)$. Without an external trapping potential, the impurity density is constant in the absence of self-localization, $\rho_I(x_0) = \frac{1}{\Omega}$, while in the presence of self-localization $\rho_I(x_0)$ peaks at a random location \bar{x}_0 ¹ and falls to zero away from \bar{x}_0 . Similarly, the density of the Bose gas $\rho_B(x_1)$ is constant in the first case, $\rho_B(x_1) = \frac{N}{\Omega}$, while it has a valley/peak for repulsive/attractive impurity-boson interaction in the latter case. For the correlated polaron ansatz (3), the impurity density is given by

$$\rho_I(x_0) = \int dx_1 \dots dx_N |\Psi|^2 = \eta(x_0)^2 \bar{f}(x_0)^N, \quad (8)$$

and the boson density is given by

$$\begin{aligned} \rho_B(x_1) &= N \int dx_0 dx_2 \dots dx_N |\Psi|^2 \\ &= \frac{N}{\Omega} \int dx_0 \eta(x_0)^2 \bar{f}(x_0)^{N-1} f(x_0, x_1)^2, \end{aligned} \quad (9)$$

where normalization of the wave function was assumed.

According to the Ritz variational principle the optimal $\eta(x_0)$ and $f(x_0, x_1)$ are obtained from minimizing the energy

(7), i.e., setting its functional derivatives with respect to $\eta(x_0)$ and $f(x_0, x_1)$ to zero. To ensure normalization of the wave function we introduce a Lagrange multiplier λ . Hence, we need to optimize the Lagrangian

$$L = E + \lambda \left\{ 1 - \int dx_0 \eta(x_0)^2 \bar{f}(x_0)^N \right\}. \quad (10)$$

The inh-CP equations for the general inhomogeneous case are the coupled Euler-Lagrange equations, formally written as

$$\frac{\delta L}{\delta \eta(x_0)} = 0, \quad (11)$$

$$\frac{\delta L}{\delta f(x_0, x_1)} = 0. \quad (12)$$

Their explicit form is derived in Appendix A, where we show that in the thermodynamic limit $N \rightarrow \infty$ and $\Omega \rightarrow \infty$ with $\rho = \frac{N}{\Omega}$ fixed, we obtain a one-body equation for the square root of the impurity density $g(x_0) = \sqrt{\rho_I(x_0)}$ and a two-body equation for $\tilde{f}(x_0, x_1) \equiv g(x_0)f(x_0, x_1)$:

$$\mu_I g(x_0) = -\frac{\hbar^2}{2M} \frac{\partial^2 g(x_0)}{\partial x_0^2} + V_g(x_0) g(x_0), \quad (13)$$

$$\mu_B \tilde{f}(x_0, x_1) = -\frac{\hbar^2}{2M} \frac{\partial^2 \tilde{f}(x_0, x_1)}{\partial x_0^2} - \frac{\hbar^2}{2m} \frac{\partial^2 \tilde{f}(x_0, x_1)}{\partial x_1^2} + V_f(x_0, x_1) \tilde{f}(x_0, x_1) \quad (14)$$

with the impurity and boson chemical potential μ_I and μ_B and the effective one-body and two-body potentials

$$\begin{aligned} V_g(x_0) &= \frac{\hbar^2}{2M} \rho \int dx'_1 \left(\frac{\partial f(x_0, x'_1)}{\partial x_0} \right)^2 + \frac{\hbar^2}{2m} \rho \int dx'_1 \left(\frac{\partial f(x_0, x'_1)}{\partial x'_1} \right)^2 + \rho \int dx'_1 f(x_0, x'_1)^2 U(x_0, x'_1) \\ &+ \lambda_{BB} \frac{\rho^2}{2} \int dx'_1 (f(x_0, x'_1)^4 - 2 f(x_0, x'_1)^2 + 1), \end{aligned} \quad (15)$$

$$V_f(x_0, x_1) = \frac{\hbar^2}{2M} \frac{1}{g(x_0)} \frac{\partial^2 g(x_0)}{\partial x_0^2} + U(x_0, x_1) + \lambda_{BB} \rho \frac{\tilde{f}(x_0, x_1)^2}{g(x_0)^2}. \quad (16)$$

We have cast the two coupled inh-CP equations into the form of a one- and a two-body nonlinear Schrödinger equation, respectively, with effective potentials (15) and (16) that depend on $g(x_0)$ and $\tilde{f}(x_0, x_1)$ itself. Similarly to other nonlinear Schrödinger equations [39], Eqs. (13) and (14) can be solved self-consistently by imaginary time propagation, where we always start the propagation with self-localized trial states, for example, the MF ground state. Details are given in Appendix B.

III. RESULTS

We present results for the Bose polaron ground state in one dimension for three levels of approximation:

(a) Solving the full inh-CP equations (13) and (14), derived in this work and based on the ansatz (3)

(b) Solving the special case of the hom-CP equation, derived in Ref. [32], based on the ansatz (4), that precludes self-localization

(c) Solving the MF equations, based on the ansatz (2), which according to Ref. [14] always result in self-localization in one dimension.

In all three types of calculations, we use the same Gaussian interaction model. Following Bruderer *et al.* [14], we measure length in units of the healing length $\xi = \hbar/\sqrt{\lambda_{BB}\rho m}$ and energy in units of $E_0 = \lambda_{BB}\rho$. This leaves us with three dimensionless essential parameters characterizing the Bose polaron system (1): the mass ratio $\alpha = m/M$, the relative interaction strength $\beta = \lambda_{IB}/\lambda_{BB}$, and a density parameter $\gamma = 1/(\rho\xi)$. λ_{IB} is obtained from the scattering length a_{IB} via $\lambda_{IB} = -\hbar/a_{IB}(1/M + 1/m)$, and the scattering length a_{IB} is obtained from the parameters U_0 and σ_U the Gaussian model interaction using the results of Ref. [40]. We have confirmed

¹For numerical reasons, the impurity self-localizes at $\bar{x}_0 = 0$ if at all.

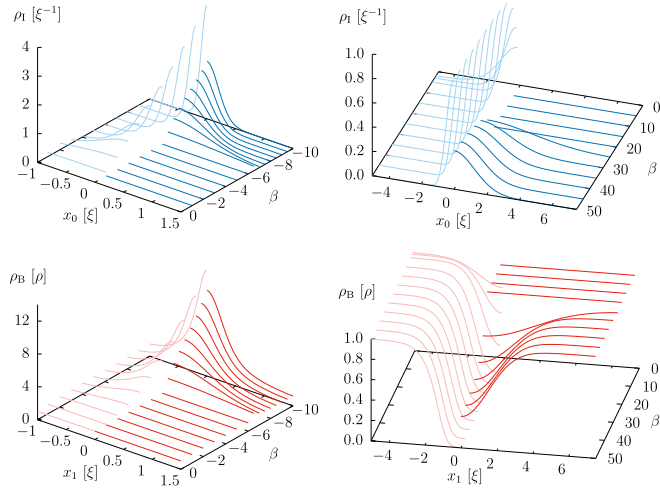


FIG. 1. Impurity density $\rho_I(x_0)$ (top panels) and boson density $\rho_B(x_1)$ (bottom panels) are shown as functions of β . Correlated polaron results are depicted on the positive side of the coordinate axis x_0 or x_1 , and the MF results are depicted on the negative side. The left and right panels show results for attractive and repulsive impurity-boson interactions, respectively. A constant $\rho_I(x_0)$ and $\rho_B(x_1)$ means there is no self-localization for the corresponding value of β . All results are for $\gamma = 0.5$.

the universality of the interaction model, i.e., that our results depend only on λ_{IB} and not on the parameters U_0 and σ_U if σ_U is chosen very small. Too small values for σ_U would require a very fine discretization and correspondingly high numerical effort. Therefore, we choose $\sigma_U = 0.1$, where results differ only insignificantly from the universal limit.

We compare results obtained with the inh-CP and the hom-CP equations to ensure numerical consistency, and also to calculate the formation energy (called binding energy in Ref. [11]) gained from self-localization if we do find self-localized polarons. But the main goal of this work is to compare the inh-CP results and MF results, i.e., results with and without including correlations, to see whether self-localization still occurs when impurity-boson correlations are included in the variational ansatz. We note that both solving the hom-CP equation and solving the MF equations is numerically straightforward and fast since all quantities depend on a single coordinate, unlike $f(x_0, x_1)$ in the inh-CP ansatz (3).

In this work we restrict ourselves to equal impurity and boson mass, i.e., $\alpha = 1$. The parameter γ is related to the gas parameter, $\rho|a_{BB}| = 2/\gamma^2$. A small parameter γ signifies weak boson-boson interactions (i.e., large $|a_{BB}|$) and/or high density, while $\gamma \rightarrow \infty$ is the strongly correlated Tonks-Girardeau limit [41]. We study two cases, $\gamma = 0.2$ and $\gamma = 0.5$, which both correspond to a weakly interacting Bose gas, where it may be justified to neglect boson-boson correlations as done in the ansatz (3). We vary the relative impurity-boson interaction strength β over a wide range from strongly attractive to strongly repulsive.

A. Density and localization length

In Fig. 1 we show the impurity density $\rho_I(x_0)$ (top panels) and the boson density $\rho_B(x_1)$ (bottom panels) for attractive

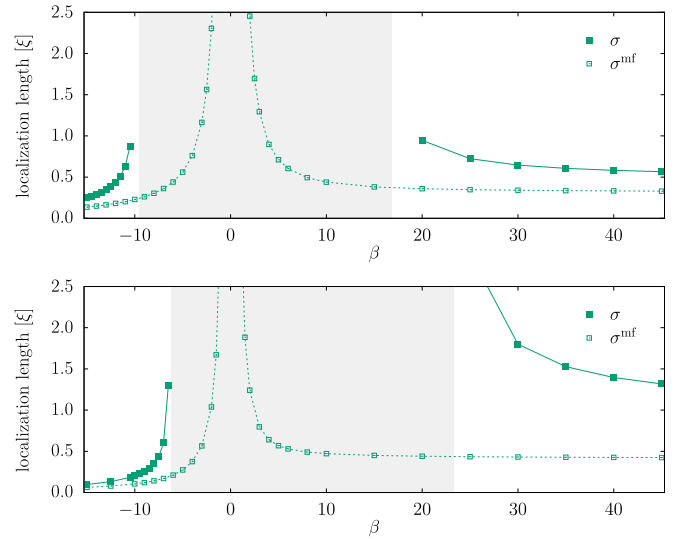


FIG. 2. Localization length σ of a polaron is plotted as a function of β for $\gamma = 0.2$ (top panel) and 0.5 (bottom panel). The filled and open symbols are the correlated and MF results, respectively, the latter agreeing with Ref. [14]. The shaded area indicates the range of β where no self-localization occurs according to our correlated results.

impurity-boson interactions, $-10 \leq \beta < 0$, (left panels) and repulsive interaction $0 < \beta \leq 50$ (right panels). We show only half of the densities since they are assumed to be symmetric. The darker lines (positive coordinates) are the solutions of the inh-CP equations, while the lighter lines (negative coordinates) are the solutions of the MF equations, calculated also in Ref. [14]. All calculations in Fig. 1 are done for $\gamma = 0.5$.

The comparison in Fig. 1 demonstrates that incorporating the impurity-boson correlations strongly reduces the tendency towards self-localization. The MF approximation predicts that the polaron self-localizes for *all* values of β , where $\rho_I(x_0)$ and $\rho_B(x_1)$ becomes narrower for larger $|\beta|$ [14]. Conversely, the ground state of the correlated polaron is qualitatively and quantitatively quite different: for a wide β range the polaron does not self-localize at all, thus $\rho_I(x_0)$ and $\rho_B(x_1)$ are simply constant. It may come as a surprise that especially for weak interactions the MF approximation gives a wrong result regarding the question of self-localization, which demonstrates that in one dimension correlations should never be neglected. Only for sufficiently strong attraction or repulsion, the correlated polaron self-localizes, but both $\rho_I(x_0)$ and $\rho_B(x_1)$ are significantly broader than in the MF approximation.

A localized polaron can be characterized by a localization length σ , e.g., by fitting a Gaussian $\exp[-x_0^2/(2\sigma^2)]/(\sigma\sqrt{2\pi})$ to the impurity densities $\rho_I(x_0)$ shown in Fig. 1. $\sigma \rightarrow \infty$ means the polaron delocalizes. In Fig. 2 we show the localization length σ of the correlated polaron (filled squares) and the corresponding σ^{mf} of the MF polaron (open squares) as functions of the relative interaction strength β for $\gamma = 0.2$ (top) and $\gamma = 0.5$ (bottom). Since in all our calculations, including the MF calculations, we use a Gaussian interaction of finite width $\sigma_U = 0.1$ instead of a contact potential, our results for σ^{mf} deviate slightly from Ref. [14], at most by

TABLE I. The critical relative interaction strengths $\beta_{\text{cr},1/2}$ for self-localization, obtained from solving the inh-CP equations. We also tabulate the results expressed in alternative dimensionless units (see text) for better comparison with Ref. [27].

γ	$\beta_{\text{cr},1}$	$\beta_{\text{cr},2}$	γ_{P}	$\eta_{\text{cr},2}$	$\eta_{\text{cr},2}$
0.2	-9.6	16.8	0.04	-0.38	0.67
0.5	-6.2	23.3	0.25	-1.55	5.82

10%. Since the MF approximation predicts unconditional self-localization in one dimension, σ^{mf} is finite for all $\beta \neq 0$. For the correlated polaron, we get a large range of β where the polaron is delocalized, indicated by the gray area. Therefore, not only is σ significantly larger than σ^{mf} , but it diverges at a critical attractive and repulsive relative interaction strength $\beta_{\text{cr},1}$ and $\beta_{\text{cr},2}$, respectively, the value of which depends on γ . Since a large σ requires a large computational domain, approaching the critical β becomes numerically expensive, and we estimate it by fitting to $a_1|\beta - \beta_{\text{cr},1}|^{c_1}$ for the attractive side and $a_2|1 - \beta_{\text{cr},1}/\beta|^{c_2}$ for the repulsive side (where σ seems to saturate at a finite value for large β). The estimates are tabulated in Table I. The Bose polaron in one dimension was studied with diffusion Monte Carlo simulations [27,28]. The trial wave functions used in that work are translationally invariant, which may mask a self-localization effect. Nonetheless, a relatively sharp increase of the polaron effective mass to a very large value was observed on both the attractive and repulsive side. Parisi *et al.* [27] considered equal masses for impurity and bosons, which allows comparison with the present work. They use the parameters $\gamma_{\text{P}} = \gamma^2$ and $\eta = \beta\gamma^2$ to characterize boson density/interactions and impurity-boson interactions, respectively. For better comparison Table I provides the critical interaction strength also in terms of γ_{P} and η . The closest values of γ_{P} compared to our values are $\gamma_{\text{P}}^{(\text{MC})} = 0.02$ and 0.2 . Figure 4 in Ref. [27] shows that for $\gamma_{\text{P}}^{(\text{MC})} = 0.02$ the inverse effective mass essentially vanishes for $\eta \approx -1$ and for $\eta \approx 1$ for attractive and repulsive interactions, respectively; for $\gamma_{\text{P}}^{(\text{MC})} = 0.2$ the corresponding values are $\eta \approx -2$ and $\eta \approx 10$, but the statistical fluctuations and the logarithmic scale make it hard to give precise numbers. Considering this uncertainty and our slightly different values for γ_{P} , our prediction for the critical interaction strength for a self-localized polaron ground state is consistent with that for an essentially infinite effective mass obtained with diffusion Monte Carlo.

B. Chemical potential

Solving the correlated polaron equations (13) and (14) yields not only $g(x_0)$ and $\tilde{f}(x_0, x_1)$ but also the impurity and boson chemical potentials μ_I and μ_B . For the latter we obtain the trivial result $\mu_B/E_0 = 1$, i.e., the MF approximation of the pure Bose gas, which is not altered by a single impurity in the thermodynamic limit. Slight numerical deviations from unity provide a measure of finite size effects.

The impurity chemical potential μ_I provides nontrivial information. According to the Ritz variational principle, better variational wave functions yield lower energies, closer to the

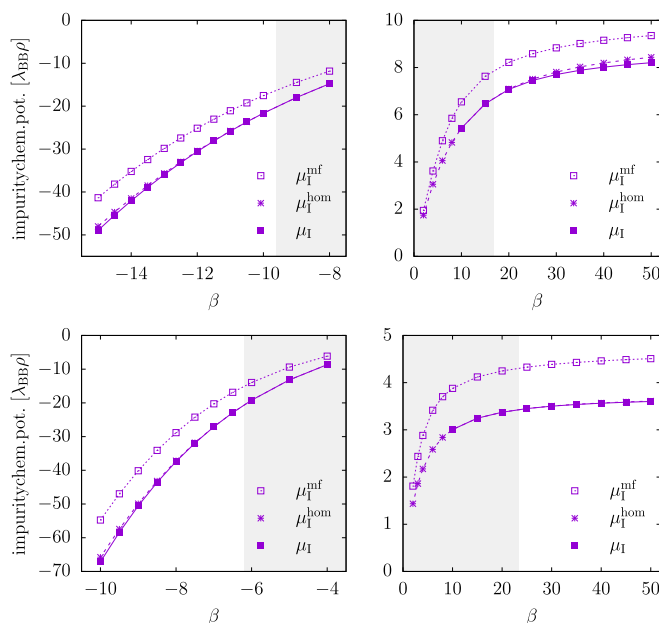


FIG. 3. Impurity chemical potential μ_I (filled squares) from the solution of the inhomogeneous correlated polaron equations is plotted as a function of β for $\gamma = 0.2$ (top panels) and 0.5 (bottom panels), together with the MF prediction μ_I^{mf} (open squares) and the homogeneous correlated polaron prediction μ_I^{hom} (stars). Left and right panels show attractive and repulsive impurity-boson interactions, respectively.

exact ground-state energy. This is also true for μ_I , because it is obtained by subtracting the constant $E_{0,N}$ from the ground-state energy; see Appendix A. Hence, the chemical potential of the correlated impurity must be lower than that of the MF impurity, $\mu_I < \mu_I^{\text{mf}}$. In Fig. 3 we show μ_I and μ_I^{mf} as functions of β for $\gamma = 0.2$ (top panels) and 0.5 (bottom panels). For all cases, μ_I^{mf} is higher than μ_I , as it should be. Furthermore, we expect $\mu_I < 0$ for $\beta < 0$ and vice versa, which is indeed the case for both μ_I and μ_I^{mf} . For attractive impurity-boson interactions, shown in the left panels, μ_I shows no sign of saturating to a finite value when β is decreased to stronger attraction; in fact, the slope steepens. For repulsive interactions (right panels), μ_I does saturate with increasing β . This is consistent with the behavior of the localization length shown in Fig. 2 for negative and positive β .

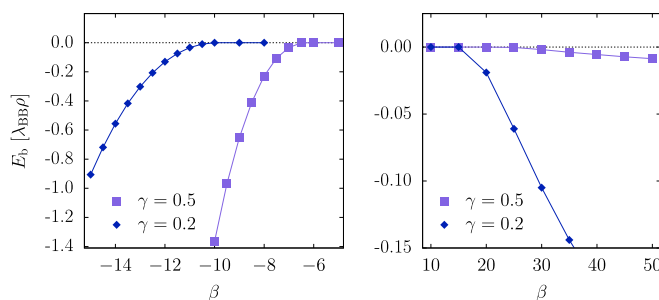


FIG. 4. Formation energy $E_b = \mu_I - \mu_I^{\text{hom}}$ is plotted as a function of β , split into attractive and repulsive interaction (left and right panel). self-localization happens only if $E_b < 0$.

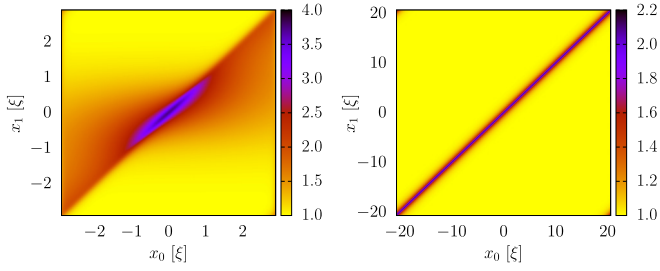


FIG. 5. Optimal pair correlation $f(x_0, x_1)$ obtained from solving the inhomogeneous correlated polaron equations. For $\beta = -10$ (left panel) the polaron ground state is self localized, and for $\beta = -5$ (right panel) the ground state is homogeneous. The values at the upper left and lower right corners of the computational domain are a result of the periodic boundary conditions.

The comparison between μ_I and μ_I^{mf} serves mainly as a check that we did not converge to an unphysical local energy minimum. More interesting is the comparison of the chemical potentials obtained from the inhomogeneous and the *homogeneous* polaron equations, μ_I and μ_I^{hom} , respectively, because the difference is the formation energy of self-localization, $E_b = \mu_I - \mu_I^{\text{hom}}$, i.e., the energy gained by localization. μ_I^{hom} is shown in Fig. 3 together with μ_I and μ_I^{mf} , but the difference between μ_I and μ_I^{hom} is barely visible. In Fig. 4 we show the formation energy E_b , which is about two orders of magnitude smaller than μ_I , and its determination without numerical bias is challenging. We note that the smallness of E_b relative to μ_I would render its calculation by Monte Carlo simulation a formidable task.

If $\mu_I = \mu_I^{\text{hom}}$, thus $E_b = 0$, no energy is gained from self-localization, which therefore does not happen. Indeed, in these cases the inh-CP solver converges to a constant polaron density, $\rho_I = 1/\Omega$, with the same correlation function $f(x_0, x_1)$ as that of the hom-CP solution, $f^{\text{hom}}(x_0 - x_1)$. If $\mu_I < \mu_I^{\text{hom}}$, thus $E_b < 0$, self-localization lowers the ground state with respect to a homogeneous ground state. The critical relative interaction strength $\beta_{\text{cr},1}$ and $\beta_{\text{cr},2}$ discussed above is just the point where E_b becomes 0.

We illustrate the difference between a homogeneous pair correlation $f^{\text{hom}}(x_0 - x_1)$ of a delocalized ground state and the inhomogeneous pair correlation $f(x_0, x_1)$ of a self-localized ground state in Fig. 5 for $\gamma = 0.5$. The left panel shows $f(x_0, x_1)$ for $\beta = -10$ (localized), which has only inversion symmetry. The right panel shows $f(x_0, x_1) = f^{\text{hom}}(x_0 - x_1)$ for $\beta = -5$ (homogeneous), which has translation symmetry with respect to the center of mass $(x_0 + x_1)/2$.

IV. CONCLUSIONS

We revisited the self-localization problem of an impurity in a Bose gas, where the mean-field (MF) approximation predicted self-localized polaron ground states in three dimensions [11] and later in two and one dimension [14]; in particular, in one dimension self-localization was predicted to happen for any strength of the impurity-boson interaction, quantified by the parameter β . Extending the MF method using the Bogoliubov method to account for quantum fluctuations has proven useful in many instances

(dipolar interactions [42], self-bound Bose mixtures [43]), but is still only a perturbative expansion. In our work, we incorporate optimized, inhomogeneous impurity-boson correlations in a nonperturbative way and derive inhomogeneous correlated polaron (inh-CP) equations, which we solve numerically for the 1D case. The results of this improved variational ansatz for the ground-state wave function shows that the MF approach is not sufficient to study polaron physics in one dimension. Impurity-boson correlations suppress the tendency towards self-localization significantly, which happens only for strongly attractive or repulsive impurity-boson interactions. Despite being variational, our results are consistent with the sharp increase of the effective mass of the polaron at a similar critical impurity-boson interaction strength predicted by exact diffusion Monte Carlo simulations [27].

In the case of the MF approximation, it is straightforward to see why it might predict a spurious self-localization even for weak interactions: without correlations, i.e., using a Hartree ansatz (2), a localized impurity density and accordingly an inhomogeneous Bose density “mimic” the effect of a correlations as the most optimal solution of the Ritz variational problem. For example, for repulsive interactions the Bose density is suppressed around the localized impurity, lowering the total energy of a Hartree ansatz. Instead, in a correlated many-body wave function like (3), repulsion causes a correlation hole in the pair distribution function, which does not require self-localization of the polaron. Our method predicts self-localization only for strong impurity-boson interactions, but this is not a rigorous proof that such a breaking of the translational invariance of the Hamiltonian (1) is a real effect rather than a variational artifact. Further refinements beyond the variational wave function (3), such as boson-boson correlations or three body impurity-boson-boson correlations, may push the transition to self-localization to even stronger interactions. However, the above-mentioned consistency with exact Monte Carlo results lends credibility to the correlated polaron ansatz (3) in the regime of weak boson-boson interactions that we studied in this work.

Experimental observation of a possibly self-localized polaron is challenging. The smallness of the formation energy E_b would require a low temperature, depending on the magnitude of $|\beta|$, where strongly attractive interactions, $\beta < 0$, are clearly favorable according to our results. Diffusion Monte Carlo simulations would in principle allow us to calculate E_b from the difference of the ground-state energies obtained from homogeneous and self-localized polaron trial wave functions, respectively, the latter coming, e.g., from our inh-CP solution. However, the smallness of E_b again makes this a challenging task.

In higher dimensions, there is no evidence of a sharp increase of the effective mass of a polaron three dimensions, according to quantum Monte Carlo simulations [25], but the MF approach [11] does predict self-localization. Correlations tend to be less important in higher dimensions, and the MF approach usually becomes a better approximation. It will be interesting to see if there is a parameter regime where the correlated polaron ansatz (3) is self localized in more than one dimension. Furthermore, the inh-CP method can be generalized to time-dependent problems, similarly to the time-dependent hypernetted-chain Euler-Lagrange method [44].

This allows us to calculate the effective mass for a direct comparison with exact Monte Carlo results or one of the many other methods used for the 1D polaron problem [45,46], but also to study nonequilibrium dynamics of polarons after a quench [47,48], such as an interaction quench of β .

Our results pertain only to neutral atomic impurities. For dipolar and especially ionic impurities, which interact via long-ranged attractive potentials with the surrounding Bose gas due to induced dipoles, the situation may be different. Ions in Bose-Einstein condensates can dress themselves with a substantial cloud of bosons [49], making ionic polarons a more likely candidate for self-localization.

ACKNOWLEDGMENTS

We thank Gregory Astrakharchik and David Miesbauer for fruitful discussions. Supported by Johannes Kepler University Open Access Publishing Fund and the federal state of Upper Austria.

APPENDIX A: DERIVATION OF THE INHOMOGENEOUS CORRELATED POLARON EQUATIONS

From the energy (7) and the resulting Lagrangian (10) we derive the inh-CP equations (13) and (14). The first Euler-Lagrange equation (11) becomes, after dividing by $2\bar{f}(x_0)^N$,

$$\begin{aligned} \lambda \eta(x_0) = & -\frac{\hbar^2}{2M} \left\{ \frac{\partial^2 \eta(x_0)}{\partial x_0^2} + 2 \frac{N}{\Omega} \frac{\partial \eta(x_0)}{\partial x_0} \frac{1}{\bar{f}(x_0)} \int dx'_1 f(x_0, x'_1) \frac{\partial f(x_0, x'_1)}{\partial x_0} \right. \\ & + \frac{N}{\Omega} \frac{\eta(x_0)}{\bar{f}(x_0)} \int dx'_1 f(x_0, x'_1) \frac{\partial^2 f(x_0, x'_1)}{\partial x_0^2} + \frac{N(N-1)}{\Omega^2} \frac{\eta(x_0)}{\bar{f}(x_0)^2} \left[\int dx'_1 f(x_0, x'_1) \frac{\partial f(x_0, x'_1)}{\partial x_0} \right]^2 \Big\} \\ & + \frac{\hbar^2}{2m} \frac{N}{\Omega} \frac{\eta(x_0)}{\bar{f}(x_0)} \int dx'_1 \left(\frac{\partial f(x_0, x'_1)}{\partial x'_1} \right)^2 + \frac{N}{\Omega} \frac{\eta(x_0)}{\bar{f}(x_0)} \int dx'_1 f(x_0, x'_1)^2 U(x_0, x'_1) \\ & + \frac{\lambda_{\text{BB}}}{2} \frac{N(N-1)}{\Omega^2} \frac{\eta(x_0)}{\bar{f}(x_0)^2} \int dx'_1 f(x_0, x'_1)^4. \end{aligned} \quad (\text{A1})$$

Note that, when we multiply this equation by $\eta(x_0) \bar{f}(x_0)^N$ and integrate over x_0 , we obtain $\lambda = E$, i.e., the Lagrange multiplier is indeed the energy.

Using (7) and (10), the second Euler-Lagrange equation (11) becomes, after dividing by $\frac{2N}{\Omega} \bar{f}(x_0)^{N-1}$,

$$\begin{aligned} E \eta(x_0)^2 f(x_0, x_1) = & -\frac{\hbar^2}{2M} \left\{ \eta(x_0) \frac{\partial^2 \eta(x_0)}{\partial x_0^2} f(x_0, x_1) + \eta(x_0)^2 \frac{\partial^2 f(x_0, x_1)}{\partial x_0^2} \right. \\ & + 2 \frac{N-1}{\Omega} \frac{\eta(x_0)}{\bar{f}(x_0)^{-1}} \frac{\partial \eta(x_0)}{\partial x_0} f(x_0, x_1) \int dx'_1 f(x_0, x'_1) \frac{\partial f(x_0, x'_1)}{\partial x_0} \\ & + \frac{N-1}{\Omega} \frac{\eta(x_0)^2}{\bar{f}(x_0)} f(x_0, x_1) \int dx'_1 f(x_0, x'_1) \frac{\partial^2 f(x_0, x'_1)}{\partial x_0^2} \\ & + \frac{(N-1)(N-2)}{\Omega^2} \frac{\eta(x_0)^2}{\bar{f}(x_0)^2} f(x_0, x_1) \left[\int dx'_1 f(x_0, x'_1) \frac{\partial f(x_0, x'_1)}{\partial x_0} \right]^2 + 2 \eta(x_0) \frac{\partial \eta(x_0)}{\partial x_0} \frac{\partial f(x_0, x_1)}{\partial x_0} \\ & \left. + 2 \frac{N-1}{\Omega} \frac{\eta(x_0)^2}{\bar{f}(x_0)} \frac{\partial f(x_0, x_1)}{\partial x_0} \int dx'_1 f(x_0, x'_1) \frac{\partial f(x_0, x'_1)}{\partial x_0} \right\} \\ & - \frac{\hbar^2}{2m} \left\{ \eta(x_0)^2 \frac{\partial^2 f(x_0, x_1)}{\partial x_1^2} - \frac{N-1}{\Omega} \frac{\eta(x_0)^2}{\bar{f}(x_0)} f(x_0, x_1) \int dx'_1 \left(\frac{\partial f(x_0, x'_1)}{\partial x'_1} \right)^2 \right\} \\ & + \eta(x_0)^2 f(x_0, x_1) U(x_0, x_1) + \frac{\eta(x_0)^2}{\bar{f}(x_0)} f(x_0, x_1) \int dx'_1 f(x_0, x'_1)^2 U(x_0, x'_1) \\ & + \lambda_{\text{BB}} \frac{N-1}{\Omega} \frac{\eta(x_0)^2}{\bar{f}(x_0)} f(x_0, x_1)^3 + \frac{\lambda_{\text{BB}}}{2} \frac{(N-1)(N-2)}{\Omega^2} \frac{\eta(x_0)^2}{\bar{f}(x_0)^2} f(x_0, x_1) \int dx'_1 f(x_0, x'_1)^4. \end{aligned} \quad (\text{A2})$$

We can simplify this lengthy equation by dividing by $\eta(x_0)$ and subtracting Eq. (A1) multiplied by $f(x_0, x_1)$,

$$\begin{aligned} \Delta E \eta(x_0) f(x_0, x_1) = & -\frac{\hbar^2}{2M} \left[2 \frac{\partial \eta(x_0)}{\partial x_0} \frac{\partial f(x_0, x_1)}{\partial x_0} + 2 \frac{N-1}{\Omega} \frac{\eta(x_0)}{\bar{f}(x_0)} \frac{\partial f(x_0, x_1)}{\partial x_0} \int dx'_1 f(x_0, x'_1) \frac{\partial f(x_0, x'_1)}{\partial x_0} \right. \\ & \left. + \eta(x_0) \frac{\partial^2 f(x_0, x_1)}{\partial x_0^2} \right] \\ & - \frac{\hbar^2}{2m} \eta(x_0) \frac{\partial^2 f(x_0, x_1)}{\partial x_1^2} + \eta(x_0) U(x_0, x_1) f(x_0, x_1) \\ & + \lambda_{\text{BB}} \frac{N-1}{\Omega} \frac{\eta(x_0)}{\bar{f}(x_0)} f(x_0, x_1)^2 f(x_0, x_1), \end{aligned} \quad (\text{A3})$$

where we abbreviate

$$\begin{aligned} \Delta E \equiv & -\frac{\hbar^2}{2M} \left\{ \frac{2}{\Omega} \frac{\partial \eta(x_0)}{\partial x_0} \frac{1}{\bar{f}(x_0)} \int dx'_1 f(x_0, x'_1) \frac{\partial f(x_0, x'_1)}{\partial x_0} + \frac{1}{\Omega} \frac{\eta(x_0)}{\bar{f}(x_0)} \int dx'_1 f(x_0, x'_1) \frac{\partial^2 f(x_0, x'_1)}{\partial x_0^2} \right. \\ & \left. + 2 \frac{N-1}{\Omega^2} \frac{\eta(x_0)}{\bar{f}(x_0)^2} \left[\int dx'_1 f(x_0, x'_1) \frac{\partial f(x_0, x'_1)}{\partial x_0} \right]^2 \right\} \\ & + \frac{\hbar^2}{2m} \frac{1}{\Omega} \frac{\eta(x_0)}{\bar{f}(x_0)} \int dx'_1 \left(\frac{\partial f(x_0, x'_1)}{\partial x'_1} \right)^2 + \frac{1}{\Omega} \frac{\eta(x_0)}{\bar{f}(x_0)} \int dx'_1 f(x_0, x'_1)^2 U(x_0, x'_1) \\ & + \lambda_{\text{BB}} \frac{N-1}{\Omega^2} \frac{\eta(x_0)}{\bar{f}(x_0)^2} \int dx'_1 f(x_0, x'_1)^4. \end{aligned} \quad (\text{A4})$$

By comparison with Eq. (A1), we see that ΔE is actually the difference between the energy $E = E_{1,N}$ of one impurity and N bosons (see Eq. (7)) and the energy $E_{1,N-1}$ of one impurity and $N-1$ bosons [see Eq. (7) with N decremented by 1]. Thus ΔE is the chemical potential μ_B of the Bose gas,

$$\Delta E = E - E_{1,N-1} = \mu_B. \quad (\text{A5})$$

In the thermodynamic limit of an impurity in an infinitely large bath of bosons we can simplify Eqs. (A1) and (A3) by letting $N \rightarrow \infty$ and $\Omega \rightarrow \infty$, with a constant boson density $\rho = \frac{N}{\Omega}$. This will provide a simple expression for $\bar{f}(x_0)$, Eq. (6). For large separation between the impurity and a boson, $|x_0 - x_1| \rightarrow \infty$, they are not correlated, $f(x_0, x_1) \rightarrow 1$. $h(x_0, x_1) \equiv f(x_0, x_1)^2 - 1$ provides a measure for the correlations in the sense that $h \rightarrow 0$ means no correlations. We express $\bar{f}(x_0)$ in terms of h ,

$$\begin{aligned} \bar{f}(x_0) &= \frac{1}{\Omega} \int dx_1 [1 + h(x_0, x_1)] \\ &= 1 + \frac{1}{\Omega} \int dx_1 h(x_0, x_1) = 1 + \frac{\rho}{N} \int dx_1 h(x_0, x_1). \end{aligned}$$

Clearly, $\bar{f}(x_0) \rightarrow 1$ in the thermodynamic limit $N \rightarrow \infty$, but taken to the power of N , we obtain a nontrivial function

$$\begin{aligned} \bar{f}(x_0)^N &= \left[1 + \frac{\rho}{N} \int dx_1 h(x_0, x_1) \right]^N \\ &\rightarrow \exp \left[\rho \int dx_1 h(x_0, x_1) \right]. \end{aligned} \quad (\text{A6})$$

Most of the terms in Eqs. (A1) and (A3) are proportional to $\bar{f}(x_0)^{-1}$ or $\bar{f}(x_0)^{-2}$, and one might be tempted to use $\bar{f}(x_0) \rightarrow 1$ in all of them. However, the last term on the left side of Eq. (A1) requires closer attention. With $N-1 \approx N$ this term can be written as

$$\frac{\lambda_{\text{BB}}}{2} \rho^2 \frac{\eta(x_0)}{\bar{f}(x_0)^2} \int dx'_1 f(x_0, x'_1)^4. \quad (\text{A7})$$

Because of $f(x_0, x_1) \rightarrow 1$ for $|x_0 - x_1| \rightarrow \infty$, the integral scales with the volume Ω , and we must include corrections to $\bar{f}(x_0)^{-2}$ of order $1/\Omega$. We expand $\bar{f}(x_0) = \Omega^{-1} \int dx'_1 f(x_0, x'_1)^2$ in powers of Ω^{-1} and obtain to first order

$$\bar{f}(x_0)^{-2} \approx 1 - \frac{2}{\Omega} \int dx'_1 [f(x_0, x'_1)^2 - 1]. \quad (\text{A8})$$

Thus, in the thermodynamic limit, the term (A7) becomes

$$\frac{\lambda_{\text{BB}}}{2} \rho^2 \eta(x_0) \int dx'_1 [f(x_0, x'_1)^4 - 2 f(x_0, x'_1)^2 + 2], \quad (\text{A9})$$

and Eq. (A1) can be written

$$\begin{aligned} E \eta(x_0) = & -\frac{\hbar^2}{2M} \left\{ \frac{\partial^2 \eta(x_0)}{\partial x_0^2} + 2\rho \frac{\partial \eta(x_0)}{\partial x_0} \int dx'_1 f(x_0, x'_1) \frac{\partial f(x_0, x'_1)}{\partial x_0} + \rho \eta(x_0) \int dx'_1 f(x_0, x'_1) \frac{\partial^2 f(x_0, x'_1)}{\partial x_0^2} \right. \\ & \left. + \rho^2 \eta(x_0) \left[\int dx'_1 f(x_0, x'_1) \frac{\partial f(x_0, x'_1)}{\partial x_0} \right]^2 \right\} \\ & + \frac{\hbar^2}{2m} \rho \eta(x_0) \int dx'_1 \left(\frac{\partial f(x_0, x'_1)}{\partial x'_1} \right)^2 + \rho \eta(x_0) \int dx'_1 f(x_0, x'_1)^2 U(x_0, x'_1) \\ & + \frac{\lambda_{\text{BB}}}{2} \rho^2 \eta(x_0) \int dx'_1 [f(x_0, x'_1)^4 - 2 f(x_0, x'_1)^2 + 2]. \end{aligned} \quad (\text{A10})$$

Both sides of this equation scale linearly with N . Therefore, before taking the thermodynamic limit, we subtract the MF energy of N bosons without impurity $E_{0,N} = \frac{\rho^2}{2} \lambda_{\text{BB}} \Omega$ multiplied by $\eta(x_0)$. With $E \equiv E_{1,N}$ we can then identify the impurity chemical potential $\mu_1 = E_{1,N} - E_{0,N}$ on the right-hand side of the resulting equation. Furthermore, we introduce the square root $g(x_0) = \sqrt{\rho_1(x_0)}$ of the impurity density defined in Eq. (8), which in the thermodynamic limit becomes [see Eq. (A6)]

$$\begin{aligned} \rho_1(x_0) &= \eta(x_0)^2 \bar{f}(x_0)^N \\ &= \eta(x_0)^2 \exp \left[\rho \int dx'_1 h(x_0, x'_1) \right]. \end{aligned} \quad (\text{A11})$$

This permits to write the one-body inh-CP equation in the final form given in Eq. (13).

We use $N - 1 \approx N$ and $\bar{f}(x_0) \rightarrow 1$ also in the two-body equation (A3),

$$\begin{aligned} \mu_B g(x_0) f(x_0, x_1) = & -\frac{\hbar^2}{2M} \frac{1}{g(x_0)} \frac{\partial}{\partial x_0} g(x_0)^2 \frac{\partial f(x_0, x_1)}{\partial x_0} - \frac{\hbar^2}{2m} g(x_0) \frac{\partial^2 f(x_0, x_1)}{\partial x_1^2} \\ & + g(x_0) U(x_0, x_1) f(x_0, x_1) + \lambda_{\text{BB}} \rho g(x_0) f(x_0, x_1)^2 f(x_0, x_1). \end{aligned} \quad (\text{A12})$$

The final form (14) is obtained by defining $\tilde{f}(x_0, x_1) = g(x_0) f(x_0, x_1)$.

APPENDIX B: SOLVING THE CORRELATED POLARON EQUATIONS

The correlated polaron equations (13) and (14) are coupled nonlinear integro-differential equations for which we seek the solution of lowest energy, according to the Ritz variational principle. We need a robust numerical scheme to obtain these solutions.

The one-body inh-CP equation (13) has already the convenient form of a nonlinear Schrödinger equation. But the calculation of $\frac{1}{g(x_0)} \frac{\partial^2 g(x_0)}{\partial x_0^2}$ in the effective potential (B2) in the two-body inh-CP equation (14) can be numerically challenging: if $g(x_0)$ is self localized, it decays exponentially for large x_0 . We therefore replace $\frac{1}{g(x_0)} \frac{\partial^2 g(x_0)}{\partial x_0^2}$ using the one-body equation (13) and obtain the alternative two-body equation

$$(\mu_B + \mu_1) \tilde{f}(x_0, x_1) = -\frac{\hbar^2}{2M} \frac{\partial^2 \tilde{f}(x_0, x_1)}{\partial x_0^2} - \frac{\hbar^2}{2m} \frac{\partial^2 \tilde{f}(x_0, x_1)}{\partial x_1^2} + \tilde{V}_f(x_0, x_1) \tilde{f}(x_0, x_1), \quad (\text{B1})$$

with the effective two-body potential

$$\tilde{V}_f(x_0, x_1) = V_g(x_0) + U(x_0, x_1) + \lambda_{\text{BB}} \rho \frac{\tilde{f}(x_0, x_1)^2}{g(x_0)^2}. \quad (\text{B2})$$

Note that we still have to divide $\tilde{f}(x_0, x_1)$ by $g(x_0)$ for the calculation of $V_g(x_0)$. This is the price for formulating the two-body equation as nonlinear Schrödinger equation for $\tilde{f}(x_0, x_1)$. This division by $g(x_0)$ can be problematic for localized solutions $g(x_0)$ if we choose the computation domain too large.

Equations (13) and (B1) are coupled nonlinear one- and two-body Schrödinger equations with effective Hamiltonians $H_g = T_1 + V_g$ and $H_f = T_1 + T_B + \tilde{V}_f$, containing the potentials (15) and (B2), respectively. We obtain the ground state by the imaginary time propagation. We initialize g and f at imaginary time $\tau = 0$ with localized states, e.g., a MF solution, and then use small time steps $\Delta\tau$ together with the Trotter approximation [50] to calculate an approximation of the ground state by performing a large number M of propagation steps until convergence is reached:

$$g(M\Delta\tau) = (e^{-V_g/2\Delta\tau} e^{-T_1\Delta\tau} e^{-V_g/2\Delta\tau})^M g(0), \quad (\text{B3})$$

$$\tilde{f}(M\Delta\tau) = (e^{-\tilde{V}_f/2\Delta\tau} e^{-(T_1+T_B)\Delta\tau} e^{-\tilde{V}_f/2\Delta\tau})^M \tilde{f}(0). \quad (\text{B4})$$

Between time steps we have to normalize $g(x_0)$, which is the square root of the impurity density,

$$\int dx_0 g(x_0)^2 = 1. \quad (\text{B5})$$

Furthermore, in the thermodynamic limit the impurity and bosons should be uncorrelated for large separation, i.e., $f(x_0, x_1) \rightarrow 1$ for $|x_0 - x_1| \rightarrow \infty$. In order to ensure this

property, we specifically require

$$f(x_0 = 0, x_1 \rightarrow \infty) = 1. \quad (\text{B6})$$

In summary, we perform the following calculations for each time step $\Delta\tau$ of the imaginary time propagation:

- (1) Calculate V_g (15) and \tilde{V}_f (B2)
- (2) Multiply f by g to get \tilde{f}
- (3) Multiply g by $\exp(-V_g/2\Delta\tau)$
- (4) Calculate the Fourier transform of g , multiply $g(k_0)$ by $\exp[-T_1(k_0)\Delta\tau]$ and transform back
- (5) Multiply g by $\exp(-V_g/2\Delta\tau)$
- (6) Normalize g according to Eq. (B5)
- (7) Multiply \tilde{f} by $\exp(-\tilde{V}_f/2\Delta\tau)$
- (8) Calculate the Fourier transform of \tilde{f} , multiply $\tilde{f}(k_0, k_1)$ by $\exp[-T_1(k_0)\Delta\tau - T_B(k_1)\Delta\tau]$, and transform back
- (9) Multiply \tilde{f} by $\exp(-\tilde{V}_f/2\Delta\tau)$
- (10) Divide \tilde{f} by g to get f
- (11) Normalize f according to Eq. (B6).

In steps 4 and 8, $T_1(k_0) = \frac{\hbar^2}{2M}k_0^2$ and $T_B(k_1) = \frac{\hbar^2}{2m}k_1^2$ are the Fourier transformed kinetic energies.

From the converged result, we calculate the impurity chemical potential μ_1 using the change in normalization by imaginary time propagation: we propagate one time step without normalizing $g(x_0)$ and obtain μ_1 from

$$\mu_1 = -\frac{\ln[\int dx_0 g(x_0)^2]}{2\Delta\tau}. \quad (\text{B7})$$

-
- [1] H. Fröhlich, Electrons in lattice fields, *Adv. Phys.* **3**, 325 (1954).
 - [2] B. Tabbert, H. Günther, and G. zu Putlitz, Optical investigation of impurities in superfluid ^4He , *J. Low Temp. Phys.* **109**, 653 (1997).
 - [3] J. P. Toennies and A. F. Vilesov, Superfluid helium droplets: A uniquely cold nanomatrix for molecules and molecular complexes, *Angew. Chem. Int. Ed.* **43**, 2622 (2004).
 - [4] Jan Peter Toennies, Helium nanodroplets formation, physical properties and superfluidity, in *Molecules in Superfluid Helium Nanodroplets*, edited by Alkwin Slenczka and Jan Peter Toennies, Topics in Applied Physics Vol. 145 (Springer, 2022), pp. 1–40.
 - [5] J. Catani, G. Lamporesi, D. Naik, M. Gring, M. Inguscio, F. Minardi, A. Kantian, and T. Giamarchi, Quantum dynamics of impurities in a one-dimensional Bose gas, *Phys. Rev. A* **85**, 023623 (2012).
 - [6] M.-G. Hu, M. J. V. de Graaff, D. Kedar, J. P. Corson, E. A. Cornell, and D. S. Jin, Bose polarons in the strongly interacting regime, *Phys. Rev. Lett.* **117**, 055301 (2016).
 - [7] N. B. Jorgensen, L. Wacke, K. T. Skalmstang, M. M. Parish, J. Levinsen, R. S. Christensen, G. M. Bruun, and J. J. Arlt, Observation of attractive and repulsive polarons in a Bose-Einstein condensate, *Phys. Rev. Lett.* **117**, 055302 (2016).
 - [8] L. D. Landau, On the motion of electrons in a crystal lattice, *Phys. Z. Sowjet.* **3**, 664 (1933).
 - [9] J. Jortner, N. R. Kestner, S. A. Rice, and M. H. Cohen, Study of the properties of an excess electron in liquid helium. I. The nature of the electron-helium interactions, *J. Chem. Phys.* **43**, 2614 (1965).
 - [10] D. Emin, *Polarons* (Cambridge University Press, 2013).
 - [11] F. M. Cucchiatti and E. Timmermans, Strong-coupling polarons in dilute gas Bose-Einstein condensates, *Phys. Rev. Lett.* **96**, 210401 (2006).
 - [12] R. M. Kalas and D. Blume, Interaction-induced localization of an impurity in a trapped Bose-Einstein condensate, *Phys. Rev. A* **73**, 043608 (2006).
 - [13] K. Sacha and E. Timmermans, Self-localized impurities embedded in a one-dimensional Bose-Einstein condensate and their quantum fluctuations, *Phys. Rev. A* **73**, 063604 (2006).
 - [14] M. Bruderer, W. Bao, and D. Jaksch, Self-trapping of impurities in Bose-Einstein condensates: Strong attractive and repulsive coupling, *Europhys. Lett.* **82**, 30004 (2008).
 - [15] D. H. Santamore and E. Timmermans, Multi-impurity polarons in a dilute Bose-Einstein condensate, *New J. Phys.* **13**, 103029 (2011).
 - [16] A. A. Blinova, M. G. Boshier, and E. Timmermans, Two polaron flavors of the Bose-Einstein condensate impurity, *Phys. Rev. A* **88**, 053610 (2013).
 - [17] J. Li, J. An, and C. S. Ting, Interaction-induced localization of mobile impurities in ultracold systems, *Sci. Rep.* **3**, 3147 (2013).

- [18] A. Boudjemâa, Self-localized state and solitons in a Bose-Einstein-condensate-impurity mixture at finite temperature, *Phys. Rev. A* **90**, 013628 (2014).
- [19] A. Boudjemâa, Self-consistent theory of a Bose-Einstein condensate with impurity at finite temperature, *J. Phys. A: Math. Theor.* **48**, 045002 (2015).
- [20] J. Tempere, W. Casteels, M. K. Oberthaler, S. Knoop, E. Timmermans, and J. T. Devreese, Feynman path-integral treatment of the BEC-impurity polaron, *Phys. Rev. B* **80**, 184504 (2009).
- [21] A. Novikov and M. Ovchinnikov, Variational approach to the ground state of an impurity in a Bose-Einstein condensate, *J. Phys. B: At. Mol. Opt. Phys.* **43**, 105301 (2010).
- [22] W. Casteels, J. Tempere, and J. T. Devreese, Polaronic properties of an ion in a Bose-Einstein condensate in the strong-coupling limit, *J. Low. Temp. Phys.* **162**, 266 (2011).
- [23] X. Li, R. Seiringer, and M. Leshko, Angular self-localization of impurities rotating in a bosonic bath, *Phys. Rev. A* **95**, 033608 (2017).
- [24] W. Li and S. Das Sarma, Variational study of polarons in Bose-Einstein condensates, *Phys. Rev. A* **90**, 013618 (2014).
- [25] L. A. P. Ardila and S. Giorgini, Impurity in a Bose-Einstein condensate: Study of the attractive and repulsive branch using quantum Monte Carlo methods, *Phys. Rev. A* **92**, 033612 (2015).
- [26] T. Hahn, S. Klimin, J. Tempere, J. T. Devreese, and C. Franchini, Diagrammatic Monte Carlo study of the Fröhlich polaron dispersion in two and three dimensions, *Phys. Rev. B* **97**, 134305 (2018).
- [27] L. Parisi and S. Giorgini, Quantum Monte Carlo study of the Bose-polaron problem in a one-dimensional gas with contact interactions, *Phys. Rev. A* **95**, 023619 (2017).
- [28] F. Grusdt, G. E. Astrakharchik, and E. Demler, Bose polarons in ultracold atoms in one dimension: Beyond the Fröhlich paradigm, *New J. Phys.* **19**, 103035 (2017).
- [29] I. Bloch, J. Dalibard, and W. Zwerger, Many-body physics with ultracold gases, *Rev. Mod. Phys.* **80**, 885 (2008).
- [30] L. P. Pitaevskii and S. Stringari, *Bose-Einstein Condensation* (Oxford University Press, 2003).
- [31] E. Feenberg, *Theory of Quantum Fluids* (Academic Press, 1969).
- [32] E. P. Gross, Motion of foreign body in boson systems, *Ann. Phys.* **19**, 234 (1962).
- [33] E. Krotscheck, Theory of correlated basis functions, in *Introduction to Modern Methods of Quantum Many-Body Theory and Their Applications*, Advances in Quantum Many-Body Theory Vol. 7, edited by A. Fabrocini, S. Fantoni, and E. Krotscheck (World Scientific, Singapore, 2002), pp. 267–330.
- [34] A. Polls and F. Mazzanti, Microscopic description of quantum liquids, in *Introduction to Modern Methods of Quantum Many-Body Theory and Their Applications*, Series on Advances in Quantum Many Body Theory Vol. 7, edited by A. Fabrocini, S. Fantoni, and E. Krotscheck (World Scientific, Singapore, 2002), p. 49.
- [35] M. Saarela and E. Krotscheck, Hydrogen isotope and ^3He impurities in liquid ^4He , *J. Low Temp. Phys.* **90**, 415 (1993).
- [36] E. Krotscheck, M. Saarela, K. Schörkhuber, and R. Zillich, Concentration dependence of the effective mass of ^3He atoms in $^3\text{He} - ^4\text{He}$ mixtures, *Phys. Rev. Lett.* **80**, 4709 (1998).
- [37] R. E. Zillich and K. B. Whaley, Quantum rotation of HCN and DCN in ^4He , *Phys. Rev. B* **69**, 104517 (2004).
- [38] R. E. Zillich and K. B. Whaley, Rotational spectra of methane and deuterated methane in helium, *J. Chem. Phys.* **132**, 174501 (2010).
- [39] S. A. Chin and E. Krotscheck, Fourth-order algorithms for solving the imaginary-time Gross-Pitaevskii equation in a rotating anisotropic trap, *Phys. Rev. E* **72**, 036705 (2005).
- [40] P. Jeszenszki, A. Yu. Cherny, and J. Brand, s-wave scattering length of a Gaussian potential, *Phys. Rev. A* **97**, 042708 (2018).
- [41] M. Girardeau, Relationship between systems of impenetrable bosons and fermions in one dimension, *J. Math. Phys.* **1**, 516 (1960).
- [42] A. R. P. Lima and A. Pelster, Quantum fluctuations in dipolar Bose gases, *Phys. Rev. A* **84**, 041604(R) (2011).
- [43] D. S. Petrov, Quantum mechanical stabilization of a collapsing Bose-Bose mixture, *Phys. Rev. Lett.* **115**, 155302 (2015).
- [44] M. Gartner, D. Miesbauer, M. Kobler, J. Freund, G. Carleo, and R. E. Zillich, Interaction quenches in Bose gases studied with a time-dependent hypernetted-chain Euler-Lagrange method, [arXiv:2212.07113](https://arxiv.org/abs/2212.07113).
- [45] G. Panochko and V. Pastukhov, Mean-field construction for spectrum of one-dimensional Bose polaron, *Ann. Phys.* **409**, 167933 (2019).
- [46] J. Jäger, R. Barnett, M. Will, and M. Fleischhauer, Strong-coupling Bose polarons in one dimension: Condensate deformation and modified Bogoliubov phonons, *Phys. Rev. Res.* **2**, 033142 (2020).
- [47] F. Grusdt, K. Seetharam, Y. Shchadilova, and E. Demler, Strong-coupling Bose polarons out of equilibrium: Dynamical renormalization-group approach, *Phys. Rev. A* **97**, 033612 (2018).
- [48] S. I. Mistakidis, A. G. Volosniev, N. T. Zinner, and P. Schmelcher, Effective approach to impurity dynamics in one-dimensional trapped Bose gases, *Phys. Rev. A* **100**, 013619 (2019).
- [49] G. E. Astrakharchik, L. A. P. Ardila, R. Schmidt, K. Jachymski, and A. Negretti, Ionic polaron in a Bose-Einstein condensate, *Commun. Phys.* **4**, 94 (2021).
- [50] H. F. Trotter, On the product of semi-groups of operators, *Proc. Am. Math. Soc.* **10**, 545 (1959).